Journal of Zhejiang University-SCIENCE A (Applied Physics & Engineering)
ISSN 1673-565X (Print); ISSN 1862-1775 (Online)
www.jzus.zju.edu.cn; www.springerlink.com
E-mail: jzus@zju.edu.cn

Experimental study on the construction shape-forming process and static behaviour of a double strut cable dome*

Ai-lin ZHANG[1,2,3], Chao SUN[1], Zi-qin JIANG[†‡1,2,3]

[1]*College of Architecture and Civil Engineering, Beijing University of Technology, Beijing 100124, China*

[2]*Beijing Key Laboratory of Advanced Manufacturing Technology, Beijing University of Technology, Beijing 100124, China*

[3]*Beijing Advanced Innovation Center for Future City Design, Beijing University of Civil Engineering and Architecture, Beijing 100044, China*

[†]E-mail: jzqbj2010@163.com

Received Feb. 10, 2017; Revision accepted Sept. 13, 2017; Crosschecked Jan. 26, 2018

Abstract: A double strut cable dome structural system was presented to improve the mechanical behaviour of a cable dome. This structure has good stability and is convenient to construct. To investigate its construction method and static performance, a structural model with a 6-m diameter was designed. From the nodal equilibrium equation, the calculation formulas for the prestress distribution with self-weight considered were deduced. Two types of construction methods, namely, assembling at high altitude and integral lifting, were adopted in the shape-forming process of the double strut cable dome, monitoring the internal force of the cable-strut components and the structural deformation. According to loading tests under full-span load and half-span load, the static behaviour of the structure was obtained and compared with the results from finite element analysis. Using the formulas deduced in this paper, the actual initial prestress considering self-weight for a double strut cable dome can be obtained accurately. This structure was suitable for tensioning the outer diagonal cables to apply prestress. Combined with the construction method for integral lifting, the difficulty and workload of the construction process can clearly be reduced, making the structure favourable for engineering application. Under an external load, the internal force of the ridge cables and inner diagonal cables decreases and the internal force of the other components increases. The results of the model tests were in good agreement with those of the finite element analysis.

Key words: Double strut cable dome; Force finding; Construction shape-forming process; Static behaviour; Model experiment
https://doi.org/10.1631/jzus.A1700071 **CLC number:** TU394

1 Introduction

In recent years, tensegrity systems have attracted great attention from engineers and have become popular as roofs for arenas and stadia due to their light weight and architectural impact. The cable dome was the first civil structure developed by Geiger according to Fuller (1975)'s tensegrity principle, "Islands of compression inside an ocean of tension". A typical cable dome consists of ridge cables, diagonal cables, hoop cables, vertical struts, a central tension ring, and an outer compression ring. The rigidity of the dome is the result of the self-stress equilibrium between continuous prestressed cables and individual compression struts (Hanaor, 1988; Dong and Yuan, 2008; Quagliaroli et al., 2015).

Well-known engineering applications of cable domes can be classified into two forms. One form is the Geiger type, including the Olympic Gymnastics and Fencing Hall (Geiger et al., 1986) in Seoul, Korea, Redbird Arena and Suncoast Dome (Pellegrino, 1992) in Florida, USA, Sky-parasol Cable Dome (Lee

‡ Corresponding author

* Project supported by the National Natural Science Foundation of China (No. 51608014), the Beijing Natural Science Foundation (Nos. 8174060 and 8131002), and the China Postdoctoral Science Foundation (No. 2017T100020)

ORCID: Zi-qin JIANG, https://orcid.org/0000-0001-9613-3972

et al., 2012) in Seoul, Korea, Tao-Yuan County Arena in Taiwan, China, and the National Fitness Centre (Zhang G et al., 2012) in Inner Mongolia, China. The other form is the Levy type that was applied in the Georgia Dome for the Atlanta Olympic Games (Levy, 1994; Terry, 1994), the largest existing cable dome. Other structural schemes, such as changing the layout of the components (Fu, 2005; Yuan et al., 2007; Zheng et al., 2008) or replacing flexible cables by rigid components (Ding et al., 2015; Gao et al., 2015), have also been proposed in the field of theoretical research. Application of cable domes in the construction field not only requires innovations in structural form with the advantages of novel appearance, better mechanical behaviour, and convenient construction, but also research on structural performance through theoretical analysis and model testing to provide a basis for the engineering application of a new cable dome structure.

Currently, model tests of the cable dome have been performed to study the construction method, deflection, and static and dynamic performance. Huang et al. (1999) designed a Geiger cable dome with a diameter of 5 m and studied the cable force and nodal displacement during various tension construction processes. For the project of the Inner Mongolia National Fitness Centre, Ge et al. (2012) and Zhang A et al. (2012) studied the construction method and structural performance under a designed load through scale models, providing a valuable reference for practical engineering. Kan and Ye (2008) proposed a Levy cable dome with a diameter of 4.8 m and investigated the structural response under a non-symmetrical load condition. Gao et al. (2015) designed a Geiger rigid bracing dome with a 6-m diameter, investigated the construction method for two cases (temporary support and no temporary support) and compared this dome with the results of forming analysis. Taniguchi et al. (1987) and Yamaguchi et al. (1987) both conducted model tests of Geiger cable domes, including a tension adjustment, deflection, and load test. Gasparini et al. (1989) studied the static and dynamic performance of the cable dome structure under different prestress conditions and discussed the relationship between the prestress level and structural frequency.

A double strut cable dome was proposed to improve the mechanical behaviour and construction efficiency of the cable dome. From the nodal equilibrium equation, the calculation formulas for the prestress distribution with self-weight considered were deduced. Two types of construction methods, namely, assembling at high altitude and with integral lifting, were adopted in the shape-forming process of the double strut cable dome, with monitoring of the internal force of the cable-strut components and structural deformation. By loading tests under a full-span load and half-span load, the static behaviour of the structure was obtained and compared with the results of finite element analysis.

2 Characteristics of the double strut cable dome

Typical Geiger and Levy cable domes are shown in Fig. 1. In the Geiger cable dome, there are fewer cables connected to a node, and the construction is simpler because the networks are in a wedge shape. However, there are no links between the top joints in the circumferential direction of the Geiger cable dome, resulting in poorer structural stiffness, especially in the horizontal direction (Fu, 2005). In the Levy cable dome, the horizontal stiffness is greatly improved by the triangulated networks. However, the greater number of components, especially more diagonal cables, seriously increases the workload of tension construction to apply a prestressed force to the structure as well as the difficulty of the construction of joints, weakening the economic advantages of the cable dome.

A double strut cable dome was proposed to solve the above shortcomings and improve the mechanical behaviour of the typical cable dome. The double strut cable dome is composed of ridge cables, diagonal cables, hoop cables, central strut, and diagonal struts, as shown in Fig. 2. In addition to the centre strut, all joints are connected to two diagonal struts so that the struts are continuous in a circular direction, different from the concept of tensegrity structures. The plane of the two struts is vertical to the ground, and the horizontal projections of the struts overlap with the hoop cables.

Double strut cable domes have better structural stiffness than the Geiger type because of the triangular nets of ridge cables. The number of diagonal

cables is only half that of the diagonal cables in the Levy type, so that the double strut cable dome requires less jack equipment and labour to apply prestress through tensioning diagonal cables. In addition, the struts are also connected with hoop cables in triangular nets, providing better stability to assemble and locate components during the construction shape-forming process. With the advantages of preferable stiffness and easy tension construction, the double strut cable dome is suitable for engineering application.

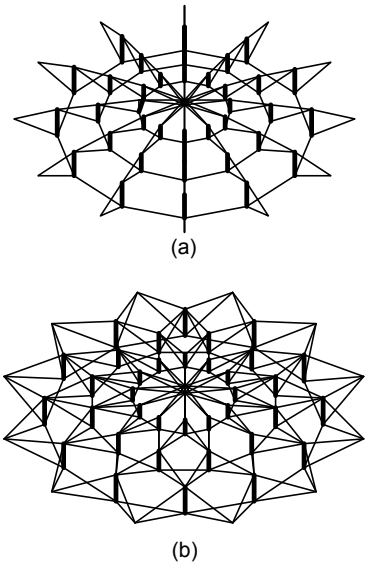

Fig. 1 Two typical cable domes
(a) Geiger type; (b) Levy type

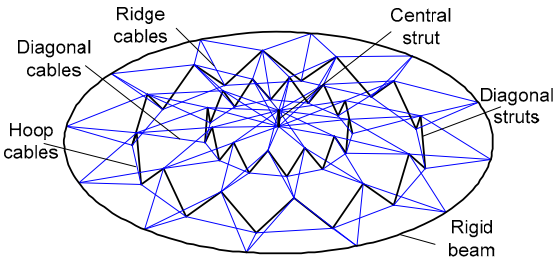

Fig. 2 3D model of a double strut cable dome

3 Simplified equations for calculating initial prestress with self-weight considered

Once the initial geometry of a cable dome is determined, the prestress design can be divided into two steps. The first step is form finding analysis to obtain the feasible prestress distribution through numerical methods, which must satisfy the equilibrium condition and symmetry possessed by the cable dome. Then, the second step is to determine the prestress level to make the structural behaviour satisfy the load conditions and design purpose. Previous research (Pellegrino, 1993; Yuan and Dong, 2003; Zhang et al., 2007; Zhou et al., 2015) on the method of form finding always relies on complex matrix operations and only calculates the ideal prestress mode without considering the self-weight of cables, struts, and joints. However, structural self-weight always exists and has an influence on the internal force and shape distribution of the structure during construction. It seems to be more meaningful to obtain the actual initial prestress with the self-weight considered to ensure that the forming state of the structure is consistent with the design. In this study, according to the balance equation of the nodes, the initial prestress formula of the double strut cable dome taking into account the structural self-weight was deduced.

Given the symmetry of the dome in polar coordinates, the structure can be divided into several equal parts along the circular direction, and for each part the distribution of components, prestress and load are the same. Considering the symmetry condition, there is only one overall feasible prestress mode in the dome, so the structure is a statically indeterminate with one redundancy. It should be noted that, for the Geiger cable dome in Fig. 1a, there are several internal mechanism displacement modes, while for the Levy type in Fig. 1b and the double strut cable dome in Fig. 2, there is no mechanism displacement mode. Therefore, similar to the Levy type, the double strut cable dome also has good stability.

Plan and profile graphs, which are used to illustrate the nodal force of the double strut cable dome, are shown in Fig. 3, wherein the struts are indicated by thick lines, ridge cables and diagonal cables are indicated by thin lines, and hoop cables are indicated by dashed lines. The numbers are 0, 1, 2, and 3 on the upper nodes from the inner ring to the outer ring, and the corresponding lower nodes are numbered 0′, 1′, 2′, and 3′. Parameter r_i is defined as the distance between node i and the centre of the cable dome. The internal

forces of the strut, ridge cable, diagonal cable, and hoop cable are expressed as S_i, R_i, D_i, and H_i, respectively. G_i and G_i' are defined as the equivalent gravity loads acting on the upper and lower nodes of the struts, which is obtained by transformation of the self-weight of the cable-strut components and joints. The variables θ_i, α_i, and β_i are defined as the angles from the strut, ridge cable, and diagonal cable to the horizontal plane, respectively, and φ_i is defined as the angle between the projective lines of the ridge cable and diagonal cable in the horizontal plane.

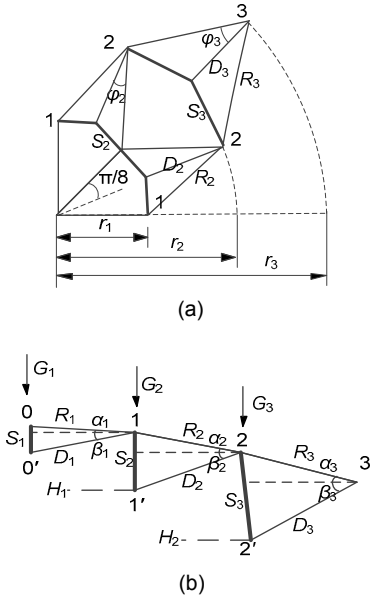

Fig. 3 Calculation graphs for the double strut cable dome
(a) Plan graph; (b) Profile graph

Equilibrium equations have been established for each node. From the internal force S_1 of the centre strut, all formulas to calculate the internal force of other components can be deduced as follows:

Node 0:

$$R_1 = \frac{-S_1 - G_1}{8\sin\alpha_1}. \tag{1}$$

Node 0′:

$$D_1 = \frac{-S_1 + G_1'}{8\sin\beta_1}. \tag{2}$$

Node 1:

$$\begin{cases} R_2 = \dfrac{1}{2\cos\alpha_2\cos(\varphi_2 + \pi/8)}(R_1\cos\alpha_1 + D_1\cos\beta_1), \\ S_2 = \dfrac{1}{2\sin\theta_2}(R_1\sin\alpha_1 - 2R_2\sin\alpha_2 - D_1\sin\beta_1 - G_2). \end{cases} \tag{3}$$

Node 1′:

$$\begin{cases} D_2 = \dfrac{-2S_2\sin\theta_2 + G_2'}{\sin\beta_2}, \\ H_1 = \dfrac{D_2\cos\beta_2}{2\sin(\pi/8)} - S_2\cos\theta_2. \end{cases} \tag{4}$$

Node 2 and Node 2′:

$$\begin{cases} R_3 = \dfrac{1}{2\cos\alpha_3\cos(\varphi_3 + \pi/8)}(2R_2\cos\alpha_2\cos\varphi_1 \\ \qquad + D_2\cos\beta_2), \\ S_3 = \dfrac{1}{2\sin\theta_3}(2R_2\sin\alpha_2 - 2R_3\sin\alpha_3 \\ \qquad - D_2\sin\beta_2 - G_3), \end{cases} \tag{5}$$

$$\begin{cases} D_3 = \dfrac{-2S_3\sin\theta_3 + G_3'}{\sin\beta_3}, \\ H_2 = \dfrac{D_3\cos\beta_3}{2\sin(\pi/8)} - S_3\cos\theta_3. \end{cases} \tag{6}$$

4 Design of test model

4.1 Design of supporting system

To investigate the construction method and static performance of the dome, a structural model was designed with a 6-m diameter and eight divisions in the circular direction. The test model consists of ridge cables (RCs), diagonal cables (DCs), hoop cables (HCs), and struts (STs). The plane, elevation view, and photograph of the test model are shown in Fig. 4, where N1, N2, and N3 are the upper nodes from the inner ring to the outer ring.

The supporting system of the test model consists of ring beams and columns, which are easy to manufacture, move, and connect. An outer ring beam was designed as an octagon composed of eight of the same I-beams, and the cross-section is H200 mm×

200 mm×12 mm×12 mm. In the middle span of each I-beam, four Φ20 mm bolts are set on the upper flange to connect to the base joints of the cable dome. A stiffener plate is welded on the web to prevent the web plate from local bucking caused by excessive concentrated force transferred from the base joints. The columns use five square steel pipes, and the cross-section is 200 mm×200 mm×20 mm×20 mm. As long as the ring beam and column sections are large enough, the supporting system maintains an adequate vertical stiffness that is sufficient to avoid any unevenness generated by the non-planeness of the ground. After finding the level, the outer ring beam is placed on the top of the square steel columns, 1 m above the ground.

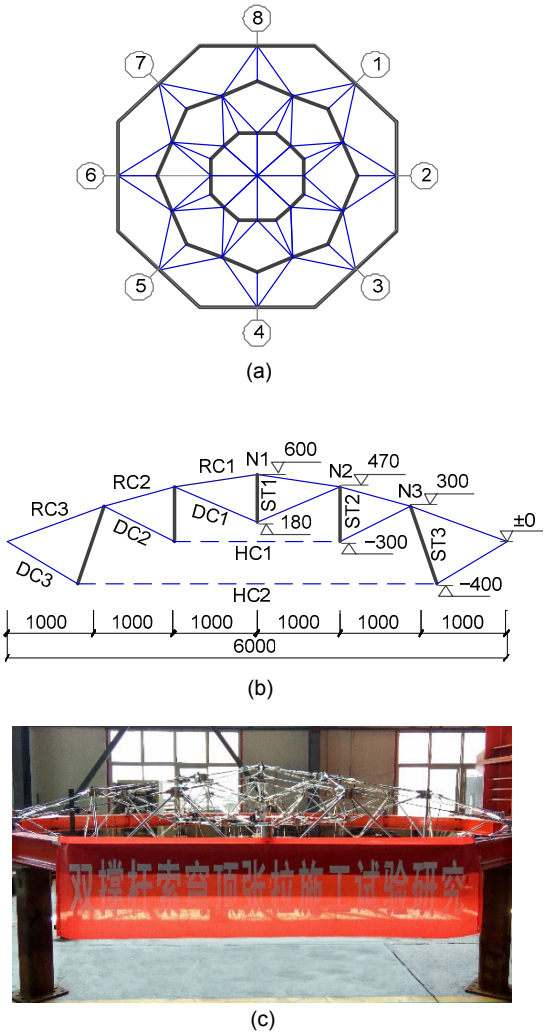

Fig. 4 Test model of a double strut cable dome
(a) Plan view; (b) Elevation view (unit: mm); (c) Model photograph

4.2 Design of the cable-strut members and joints

According to the force analysis and experimental conditions, all of the cables used Φ8 mm steel wire rope, with an adjustment sleeve at one end and an adjustable length range of ±10 mm. In the middle part of some cables, a tension sensor was connected by a threaded sleeve, as shown in Fig. 5. The compression struts used are Q345B steel pipes, and the cross-sections of ST1, ST2, and ST3 were 14 mm×3 mm, 14 mm×3 mm, and 20 mm×3 mm, respectively. The joints to connect members can be classified as the upper joints of struts, lower joints of struts, and base joints. Their construction details are shown in Fig. 6.

Fig. 5 Cables with and without a tension sensor

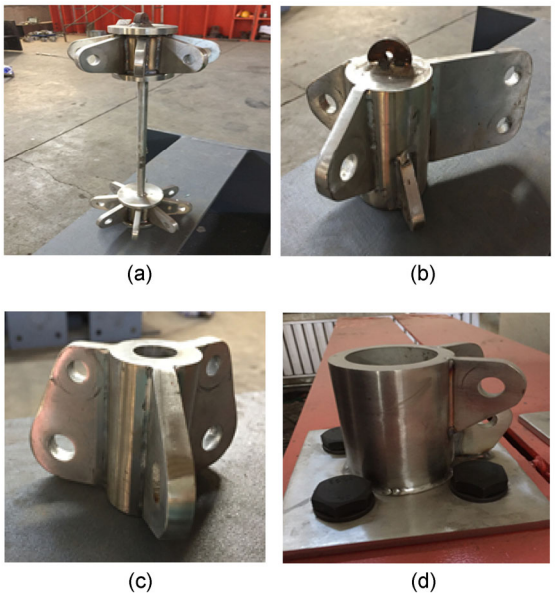

Fig. 6 Details of the joints
(a) Joint of ST1; (b) Upper joint of ST2; (c) Lower joint of ST3; (d) Base joint

To use actual material properties in finite element analysis, tensile tests were carried out on the cables and steel tubes used in the struts. The

stress-strain curves of the cable are shown in Fig. 7, and the physical properties of the steel wire rope, including Young's modulus E_s, elastic limit, failure resistance, and the two corresponding strains ε^e and ε^F, can be obtained from the curve. The physical properties of the steel tubes are shown in Table 1.

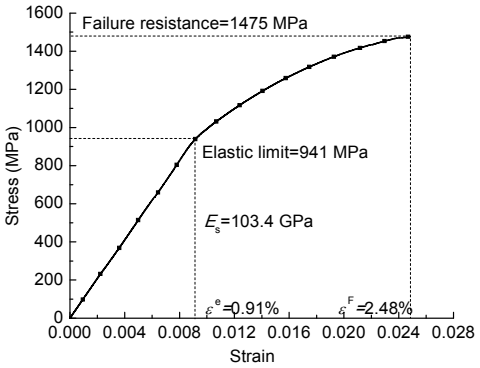

Fig. 7 Stress–strain curve of the cable elements in the structural model

Table 1 Mechanical properties of the tubes in the structural model

Tube (mm)	Elastic modulus (GPa)	Yield stress (MPa)	Ultimate stress (MPa)	Percentage elongation (%)
Φ14×3	201	332	470	19
Φ20×3	204	343	507	21

4.3 Arrangement of the measured points

This experiment focusses on changes in component force and structural shape during tension construction and static load. The cable force is monitored by BLR-1 tension transducers. The internal forces of the struts are monitored by strain gauges, and two strain gauges are arranged symmetrically at the centre of the strut. Although there is a circular symmetry in the cable dome, the distribution of internal force on each axis cannot be completely uniform in the test model. Therefore, 16 tension transducers are positioned on two opposite axes and the strain gauges are positioned on four orthogonal axes, as shown in Fig. 8a. To monitor the change in the nodal position during the forming process and thus to compare with the design value, all of the upper joints of the struts from Axis 2 to Axis 6 are taken as the monitoring points of the coordinate and measured by the total station. To obtain the vertical displacement of the structure during the loading process, three dial indicators with a gauge of 50 mm were arranged on the bottom joints of struts. The positions of the coordinate monitoring point and the dial indicators are shown in Fig. 8b.

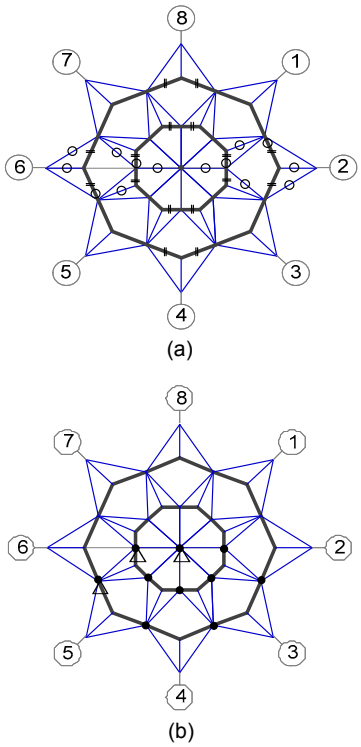

Fig. 8 Arrangement of the measured points

(a) Position of the tension sensors and strain gauges; (b) Position of the coordinate measurements and dial indicators. The symbol "○" represents the tension transducer, "=" represents the strain gauge, "●" represents the coordinate monitoring point, and "△" represents the dial indicator

4.4 Calculation of the initial prestress

Because the self-weight of the cable-strut components and joints is large and cannot be ignored, the actual prestress with self-weight considered was calculated to control the forming state of the test model. From the size of the test model shown in Fig. 4, the necessary geometric parameters in Eqs. (1)–(6) are shown in Table 2. After weighing all of the cable-strut components and joints, the equivalent gravity load acting on the node i was obtained by adding half of the sum of the component self-weight connecting node i to the joint self-weight. According to the mechanical properties of the test model under external load, the initial force of the outer hoop cable was set to 6000 N, and the internal force of the rest of the components was then calculated as shown in Table 3.

Table 2 Geometric parameters for the test model for the prestress calculation (unit: rad)

α_1	α_2	α_3	β_1	β_2	β_3
0.1293	0.1478	0.2136	0.2823	0.3452	0.4466
θ_1	θ_2	θ_3	φ_1	φ_2	φ_3
–	0.8790	0.7016	0	0.3417	0.5863

Table 3 Equivalent gravity loads and the initial prestresses of the components (unit: N)

G_1	G_1'	G_2	G_2'	G_3	G_3'
−99.15	−97.19	−59.75	−38.22	−84.78	−49.31
S_1	S_2	S_3	R_1	R_2	R_3
−1481.1	−316.3	−1368.7	1340.0	1368.3	3678.9
D_1	D_2	D_3	H_1	H_2	
708.3	1552.5	4204.5	2110.6	6000.0	

5 Test of the construction process

5.1 Construction method for assembling at high altitude

With the help of temporary support, all of the cable strut components were installed one by one at a certain height above the ground. Most of the components were installed in their original length state, namely the unstressed length before being tensioned. A few cables were chosen as active tension elements. The cable length of the active tension elements was relaxed first to facilitate their installation, and then the length was shortened by tightening the screw sleeve to simulate the tension process until their length and internal force reached the design value. Two tensioning methods (tensioning DC3 and tensioning RC3) were applied to establish the prestress in the experimental model.

The construction steps of tensioning DC3 were as follows:

(1) Erect a temporary support in the centre of the ring beam and put the ST1 on the support.

(2) Install all of the ridge cables and then install the ST2 and ST3, depending on the original length of the components.

(3) Install the DC1, DC2, HC1, and HC2, and then remove the temporary support, depending on the original length of the components.

(4) Install the DC3 and tension to the designed length in four steps. In the first step, shorten the four DC3s on the odd axes (i.e. Axes 1, 3, 5, and 7) from a length of 5 cm longer than the design value to 1 cm longer than the design value. In the second step, shorten the four DC3s on the even axes (i.e. Axes 2, 4, 6, and 8) from a length of 5 cm longer than the design value to 1 cm longer than the design value. In the third step, re-shorten the DC3s on the odd numbered axes again to the designed length. In the fourth step, re-shorten the DC3s on the even numbered axes again to the designed length. In addition, the length of DC3s tensioned in the third step may be affected slightly by the cables tensioned in the fourth step. Thus, it requires further adjustment to ensure that all lengths of DC3s meet the design requirements.

The universal finite element software program ABAQUS was used to analyse the above construction process. Truss element T3D2 was adapted to simulate the cable-strut components. To effectively consider the sag effect caused by the self-weight of the cables, the cables were divided into ten segments. The result of the tensile tests of the cable and strut components was adopted as the constitutive relations of the truss elements.

The results of the model test and numerical simulation during the construction process are shown in Fig. 9, where the internal forces of the cables and nodal coordinate are the average values of the symmetrical position. After tension forming, the measured cable force is a good match with the design value, namely, the internal forces considering the structural self-weight listed in Table 1. The maximum error in the cable force is less than 17%. The measured value of the height of the upper node in the structure is slightly lower than the design value, and their maximum difference is 7 mm.

The errors are mainly caused by the installation of a ring beam and base joints, component manufacture, instrument measurements, and the length adjustment of the active tension elements, which leads to an uneven distribution of the initial prestress. Because the strain measured in the struts is small (less than 30 με) during the construction process, there are many errors between the theoretical and the experimental results in the struts due to instrument measurement. Those data for the struts for the construction process are not listed in this paper.

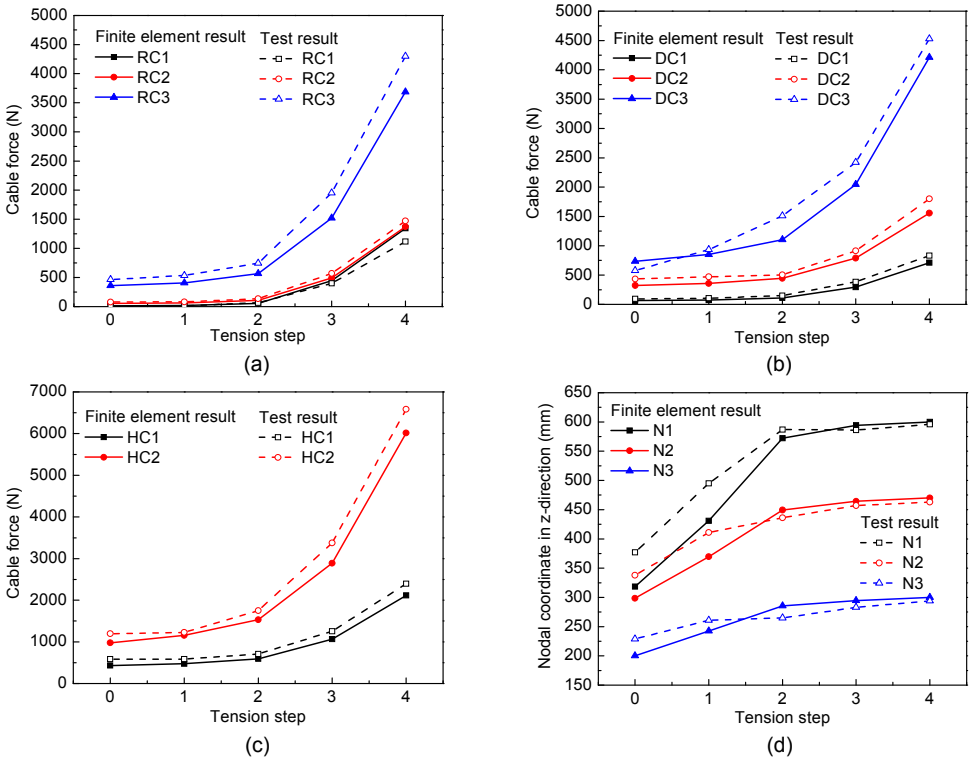

Fig. 9 Results during tensioning of DC3

(a) Internal force of the ridge cables; (b) Internal force of the diagonal cables; (c) Internal force of the hoop cables; (d) Coordinate of the upper node

The construction steps of tensioning RC3 are as follows:

(1) Erect a temporary support in the centre of the ring beam and put the ST1 on the support.

(2) Depending on the original length of the components, install all of the ridge cables and adjust the screw of RC3 to the loosest state. Then, install the ST2 and ST3.

(3) Depending on the original length of the components, install all of the diagonal cables and hoop cables. Then, remove the temporary support.

(4) Tension RC3 to the designed length in four steps. Similar to the steps for tensioning the DC3s, the RC3s on the odd axes and even axes are shortened successively, first from a length of 5 cm longer than the design value to 1 cm longer than the design value, and then, to the designed length. However, there are eight cables that need to be tensioned in each step, twice the number of tensioning the DC3.

The change of the nodal coordinate and internal force of the cables obtained by numerical simulation and the test model are shown in Fig. 10. After tension forming, the maximum error between the measured cable force and theoretical value is 21.7%, and the maximum error between the measured height of the upper node and theoretical value is 6 mm. The results of the internal force and nodal position show that, after the double construction process, the test model is in good agreement with the design and can be used as the initial state for the subsequent load test.

From the initial state and step 1 shown in Fig. 9 and Fig. 10, the measured positions of the nodes are much higher than the theoretical value. This is because most cables are in a slack state at that moment, so the cable dome structure does not have enough structural stiffness. In the test model, the slack cables have a small bending stiffness and can affect the shape and internal force distribution. However, in the finite element model, the cable elements are ideal hinged rods, and when they slacken, their contribution to structural stiffness is almost negligible.

From the final step shown in Figs. 9 and 10, the internal forces and nodal positions of the two tensioning methods are observed to be basically the same. It is proven that the two tensioning methods are both feasible for the construction of a double strut

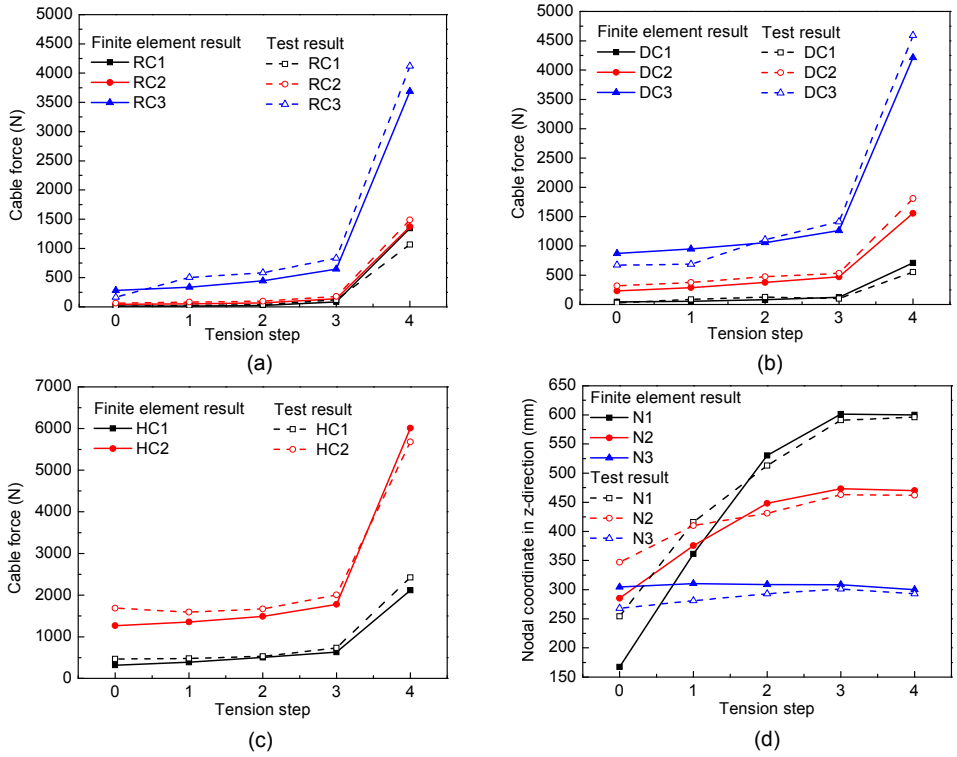

Fig. 10 Results during tensioning of RC3

(a) Internal force of ridge cables; (b) Internal force of the diagonal cables; (c) Internal force of the hoop cables; (d) Coordinate of the upper node

cable dome. As long as the length of the components can be controlled accurately, the structure can be formed by only tensioning the cables in the outer ring. However, as the number of DC3s is half of the number of RC3s, for practical engineering construction, using the method of tensioning DC3 can significantly reduce the tension equipment and workload. In addition, for a Levy cable dome with the same circular divisions, it needs to tension 16 outer diagonal cables or ridge cables to apply prestress, so the consumption of the tensioning process is much higher than that with the double strut cable dome.

5.2 Construction method for integral lifting

The construction method presented in Section 5.1 has been widely adopted in existing engineering of cable domes, but there are some shortcomings in assembling the components one by one at high altitude. Because the cable-strut components need to be installed and tensioned high above the ground, large-scale temporary supports are necessary. Those large-scale temporary supports not only increase the construction difficulty but also make it difficult to guarantee the safety of workers. Therefore, it is necessary to seek an easier and safer construction method for the double strut cable dome.

Since the cable dome does not have structural rigidity before the prestress is established, the existence of rigid body displacement obviously allows the unstable structure to deform. Therefore, an improved construction method for integral lifting can be adopted through accessory equipment such as tool cables. First, assemble all the components except for the RC3 and DC3 on the ground, then use tool cables to lift the partially assembled structure to the appropriate height, and then connect the remaining components in the outer rings (RC3 and DC3), and finally tension DC3 to complete the forming process. The detailed steps are as follows:

Step 1: Adjust all cables to their original length, except for the DC3.

Step 2: Place the ST1 on the ground in the centre of the ring beam. Connect RC1 and RC2 to ST1, connect one end of the tool cable to RC2 and connect the other end of the tool cable to the ring beam.

Step 3: Lift RC1 and RC2 to a position slightly

above the ground by tool cables to ensure that there is sufficient space to install the lower components, and then install DC1, ST2, HC1, DC2, ST3, and HC2 in turn, as shown in Fig. 11a, wherein the struts are indicated by thick lines, ridge cables and diagonal cables are indicated by thin lines, hoop cables are indicated by dashed lines, and tool cables are indicated by bold dash lines.

Step 4: Continue to lift the structure to a position slightly below the ring beam by tool cables to ensure that the upper joint of DC3 is close enough to the base joint to facilitate the installation of RC3 between the two joints, as shown in Fig. 11b.

Step 5: Gradually extend and remove the tool cables. Then the weight of whole structure borne by the tool cables is transferred to RC3, as shown in Fig. 11c.

Step 6: Connect one end of the tool cable to the lower joint of ST3 and connect the other end of the tool cable to the ring beam. Lift the structure to the appropriate height by the tool cable; then connect the DC3 between the lower joint of ST3 and the base joint. Gradually extend and remove the tool cables, as shown in Fig. 11d.

Step 7: Tension DC3 to introduce prestress to the whole structure. Monitor the length and internal force of DC3 and the node coordinates to ensure that the structure satisfies the design state, as shown in Fig. 11e.

Finite element software ABAQUS was adopted to simulate the above construction process through integral lifting. First, using the design state of the structure after tension forming, the finite element model with initial prestress was established, where the elements of eight tool cables connecting between the upper nodes of DC3 and the base nodes were also simulated by T3D2. By killing the elements of RC3 and DC3 and adjusting the length of the tool cables according to the temperature load, the structural state for the part of the structure assembled on the ground in a collapsed shape was obtained as shown in Fig. 11a. The structural state shown in Figs. 11b–11e can also be obtained in a similar way. That is, first establish the finite element model of the complete structure, then kill the elements that have not been installed or need to be removed, and finally apply a temperature load to change the length of elements that are to be tensioned or loosened in the corresponding steps. Fig. 11 also shows the coordinate of the upper nodes in each step.

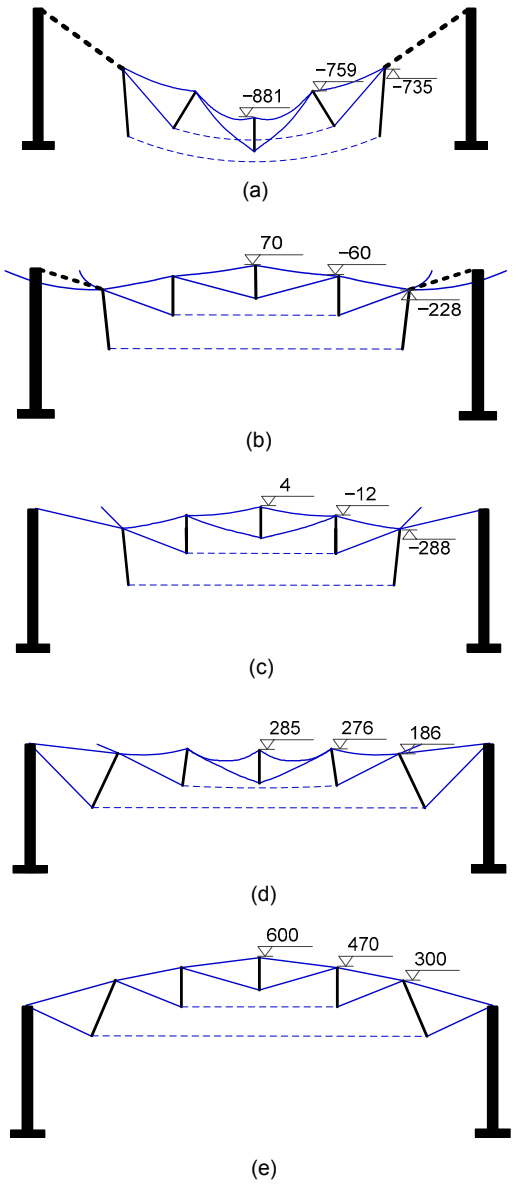

Fig. 11 Structural shape during the integral lifting construction process: (a) step 3; (b) step 4; (c) step 5; (d) step 6; (e) step 7 (unit: mm)

In the numerical simulation, the variations of the nodal height are shown in Fig. 11, and the internal forces on all components are shown in Table 4. The structural state after the forming process is observed to be in good compliance with the design objectives, indicating the feasibility and correctness of this construction method. Compared with the method described in Section 5.1, the method that proceeds through integral lifting is more suitable for practical

engineering in avoiding the complex and dangerous work of building the temporary support and connecting the components at high altitude.

Table 4 Internal forces of the components at each step

Component	Internal force (N)				
	Step 3	Step 4	Step 5	Step 6	Step 7
ST1	−87.8	−237.7	−169.8	−100.2	−1485.1
ST2	−55.1	−90.6	−78.0	−60.4	−317.0
ST3	33.6	35.1	35.1	−231.2	−1371.4
RC1	8.4	134.8	70.2	13.4	1343.5
RC2	42.3	188.9	124.6	52.4	1371.8
RC3	5.3	38.5	630.1	347.9	3687.5
DC1	43.9	149.7	117.9	62.0	710.2
DC2	230.6	522.9	461.9	312.9	1555.4
DC3	0.5	1.7	1.5	718.4	4212.5
HC1	315.4	700.3	617.1	420.1	2114.5
HC2	5.7	6.5	6.5	931.0	6011.6

6 Static loading test

6.1 Full-span loading

To study the mechanical behaviour of the double strut cable dome under static load, tests of full-span symmetrical loading and half-span asymmetric loading were carried out. The structural state including internal force and node coordinates at the beginning of static loading test is the same as the test results in Fig. 10. Since on the plane projection of the test model, the distribution area of the nodes from inner to outer is in the ratio of approximately 3:2:4; in the full-span loading test, a load is applied depending on this ratio to the upper joints of the structure. The load is divided into four stages, as shown in Table 5, and the load process is shown in Fig. 12. In the test of half-span loading, the load is also applied in four stages, but only to the upper joints of the left half region, namely, the joints between Axis 4 and Axis 8, as shown in Fig. 13. During the experiment, seventeen iron boxes were hung on the upper joints of the struts and steel blocks with specifications of 20 kg, 10 kg, and 5 kg were put in these boxes to simulate the load.

The results of the internal force of the components obtained by experiment and finite element analysis under a full-span load are shown in Fig. 14. With the increase of the load, the internal force of the ridge cables and DC1 decreases gradually and the internal force of the other cable-strut components increases gradually. In the finite element analysis, there was no cable slackening. However, after the fourth stage of loading in the model test, the slackening of RC1 occurred at Axis 2 and Axis 3, as shown in the black circles in Fig. 15, and the upper joints of ST2 connecting to these cables were inclining, as shown in the white circles in Fig. 15. The DC1 at Axis 2 also slackened, as shown in the black circle in Fig. 16. Therefore, the slackening of the inner cables could be considered to be the limit state of the structure, and the loading process was terminated.

Table 5 Loading steps on the upper joints

Step	Load (N)		
	Joint of ST1	Joint of ST2	Joint of ST3
1	150	100	200
2	300	200	400
3	450	300	600
4	500	350	700

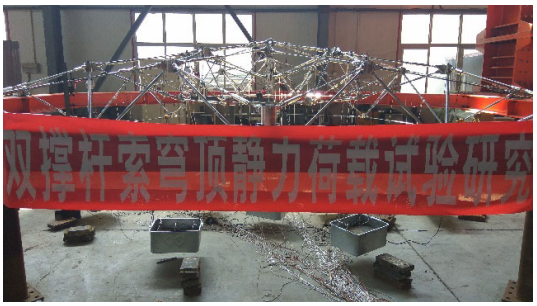

Fig. 12 Lateral view of the model under a full-span load

Fig. 13 Top view of the model under a half-span load

Before the cable slackening in the fourth stage of loading, the measured internal force of the cables and ST3 are in good agreement with their theoretical values and the maximum error is less than 20%. However, the error of internal force of ST1 and ST2 is large because the strain on these struts is relatively

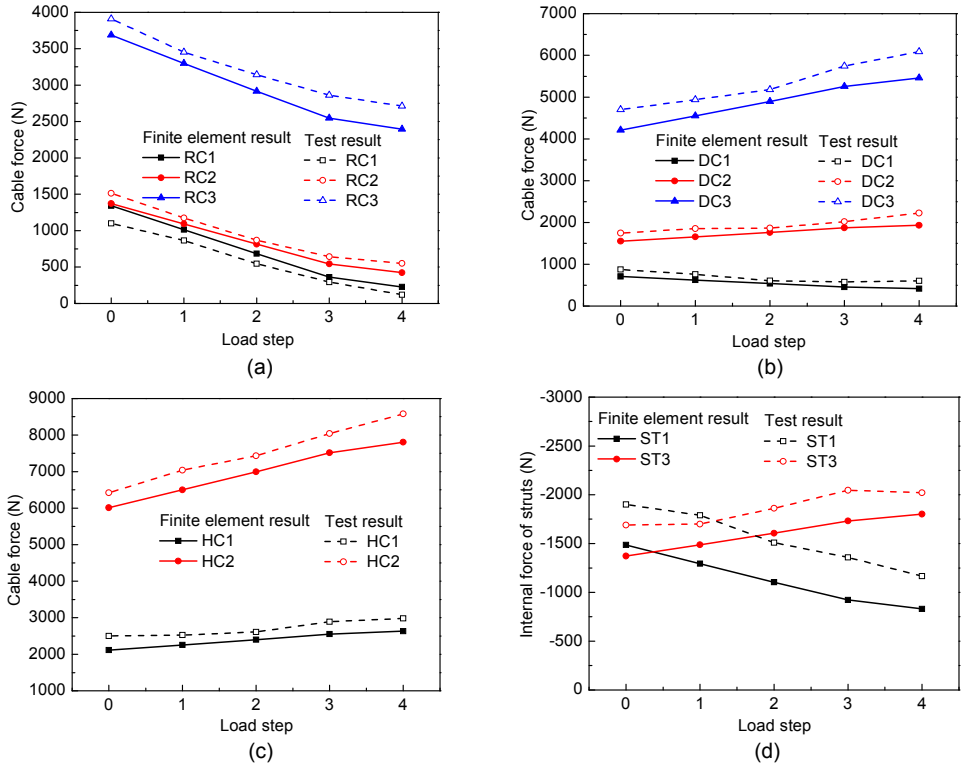

Fig. 14 Results during full-span loading

(a) Internal force of the ridge cables; (b) Internal force of the diagonal cables; (c) Internal force of the hoop cables; (d) Internal force of struts

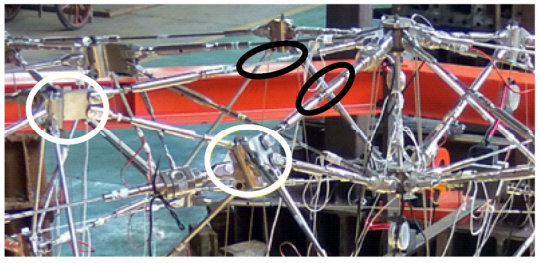

Fig. 15 Slackening of RC1 in Axes 2 and 3 and the incline of the upper node

Fig. 16 Slackening of DC1 on Axis 5

small, and some joints are loaded eccentrically during the test. After the fourth stage of loading, the errors of RC1 and DC1 reach approximately 40% because the cable slackening aggravated the eccentric loading on the joints, resulting in the increased error in the tests. The maximum vertical displacement occurs in the centre node. The reading of the dial gauge is 5.66 mm, and its theoretical value is 6.49 mm. The difference between the two is 12.8%.

6.2 Half-span loading

After the full-span loading, all components are still in the elastic state. Then the steel blocks are removed from the boxes and the inclined upper joints are adjusted until the structure approximately reaches the design state, as the start of the full-span loading test. The results of the internal force of components obtained by experiment and finite element analysis under a half-span load are shown in Fig. 17, where "L" represents the component in the left loaded region and "R" represents that in the right unloaded region. The measured results are in good agreement with the theoretical values, with a maximum difference of 16.7%. With the increase in the half-span load, the internal force on the ridge cables decreases and the internal force on the diagonal cables and hoop

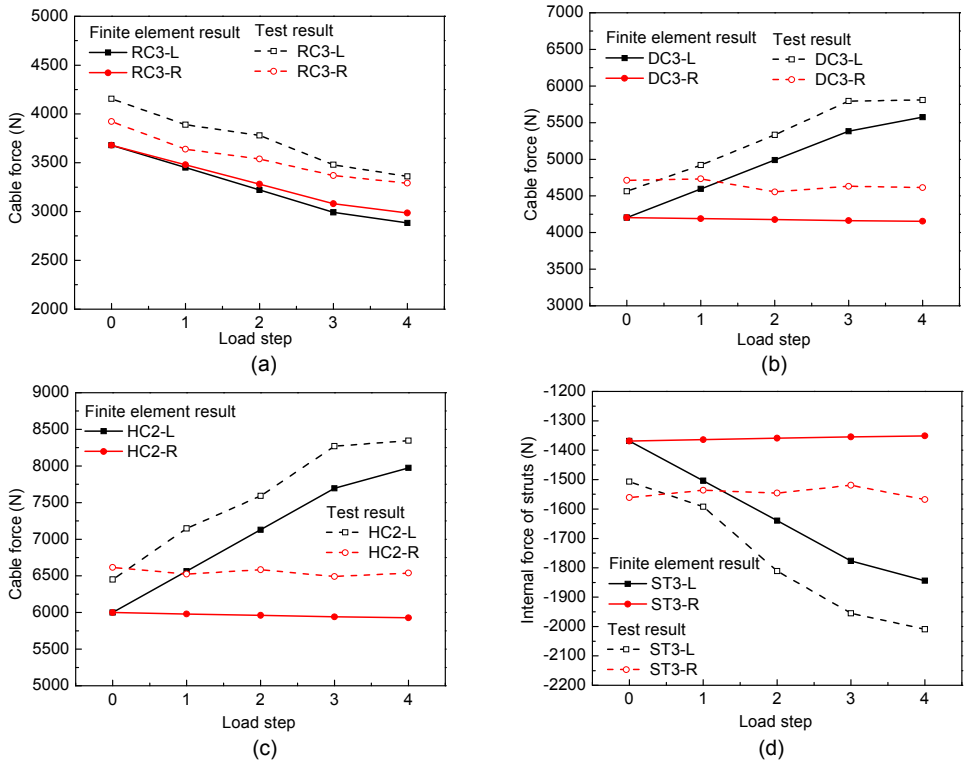

Fig. 17 Results during half-span loading

(a) Internal force of RC3; (b) Internal force of DC3; (c) Internal force of HC2; (d) Internal force of ST3

cables increases, with almost the same variation tendency as under the full-span load. However, the increase in the internal force on the diagonal cables and hoop cables is not obvious in the unloaded half-span, but their internal force increases greatly in the loaded region. The vertical displacements in the loaded and unloaded regions are 4.7 mm and 2.0 mm, respectively, both downward.

7 Conclusions

A double strut cable dome structure system has been presented. First, simplified equations for calculating initial prestress with self-weight considered were deduced. Then, a structural model with a 6-m diameter was designed to investigate the construction method and static performance through a shape-forming test and a loading test. The main conclusions are as follows:

1. The proposed formula can obtain the actual initial prestress of a double strut cable dome considering the structural weight in a simple and accurate way to ensure that the forming state of the structure is consistent with the design.

2. A double strut cable dome structure can be formed by only tensioning the cables in the outer ring. Because the number of diagonal cables is relatively small, tensioning the outer diagonal cables to apply prestress to this cable dome can significantly reduce the tension equipment and workload required.

3. The construction method that proceeded through integral lifting for the double strut cable dome was verified to be feasible and correct through finite element analysis. This method can avoid complex operation at a high altitude and greatly reduce the construction difficulty, making the double strut cable dome more suitable for practical engineering.

4. Under an external load, the internal force of the ridge cables and inner diagonal cables decreases and the internal force of other components increases. The structure reaches the limit state when the inner ridge cables or the diagonal cables slacken under a heavy load. The results of the model tests are in good agreement with those of finite element analysis.

References

Ding MM, Luo B, Guo ZX, et al., 2015. Integral tow-lifting construction technology of a tensile beam-cable dome. *Journal of Zhejiang University-SCIENCE A (Applied Physics & Engineering)*, 16(12):935-950. https://doi.org/10.1631/jzus.A1500189

Dong SL, Yuan XF, 2008. Advances in research on cable domes. *Journal of Zhejiang University (Engineering Science)*, 42(1):1-7 (in Chinese).

Fu F, 2005. Structural behavior and design methods of tensegrity domes. *Journal of Constructional Steel Research*, 61(1):23-35. https://doi.org/10.1016/j.jcsr.2004.06.004

Fuller RB, 1975. Synergetics: Explorations in the Geometry of Thinking. Macmillan Publishing Co., New York, USA.

Gao Z, Xue S, He Y, 2015a. Analysis of design and construction integration of rigid bracing dome. *Advances in Structural Engineering*, 18(11):1947-1958. https://doi.org/10.1260/1369-4332.18.11.1947

Gao Z, Xue S, He Y, et al., 2015b. Construction forming and mechanical properties test of rigid bracing dome. *Journal of Building Structures*, 36(10):29-36 (in Chinese).

Gasparini DA, Perdikaris PC, Kanj N, 1989. Dynamic and static behavior of cable dome model. *Journal of Structural Engineering*, 115(2):363-381. https://doi.org/10.1061/(ASCE)0733-9445(1989)115:2(363)

Ge J, Zhang A, Liu X, et al., 2012. Analysis of tension form-finding and whole loading process simulation of cable dome structure. *Journal of Building Structures*, 33(4):1-11 (in Chinese).

Geiger DH, Stefaniuk A, Chen D, 1986. The design and construction of two cable domes for the Korean Olympics. Proceedings of the IASS Symposium on Shells, Membranes and Space Frames, 2:265-272.

Hanaor A, 1988. Prestressed pin-jointed structures—flexibility analysis and prestress design. *Computers & Structures*, 28(6):757-769. https://doi.org/10.1016/0045-7949(88)90416-6

Huang CW, Deng Y, Song WM, 1999. Experiment analysis of cable dome structure. *Spatial Structure*, 3:40-46.

Kan Y, Ye JH, 2008. Form finding and loading experiment of cable domes. *Engineering Mechanics*, 25(8):205-211 (in Chinese).

Lee K, Han S, Park T, 2012. Stabilization process analysis of cable dome structure. *International Journal of Steel Structures*, 12(4):495-507. https://doi.org/10.1007/s13296-012-4004-4

Levy MP, 1994. The Georgia dome and beyond: achieving lightweight-longspan structures. Spatial, Lattice and Tension Structures: Proceedings of the IASS-ASCE International Symposium 1994; Held in Conjunction with the ASCE Structures Congress XII, p.560-562.

Pellegrino S, 1992. A class of tensegrity domes. *International Journal of Space Structures*, 7(2):127-142. https://doi.org/10.1177/026635119200700206

Pellegrino S, 1993. Structural computations with the singular value decomposition of the equilibrium matrix. *International Journal of Solids and Structures*, 30(21):3025-3035. https://doi.org/10.1016/0020-7683(93)90210-X

Quagliaroli M, Malerba PG, Albertin A, et al., 2015. The role of prestress and its optimization in cable domes design. *Computers & Structures*, 161:17-30. https://doi.org/10.1016/j.compstruc.2015.08.017

Taniguchi T, Ishii K, Toda I, et al., 1987. Report on experiments concerning tension dome. Proceedings of International Colloquium on Space Structures for Sports Buildings, 1:550-557.

Terry WR, 1994. Georgia dome cable roof construction techniques. Spatial, Lattice and Tension Structures: Proceedings of the IASS-ASCE International Symposium 1994; Held in Conjunction with the ASCE Structures Congress XII, p.563-572.

Yamaguchi I, Okada K, Kimura M, et al., 1987. A study on the mechanism and structural behaviors of cable dome. Proceedings of International Colloquium on Space Structures for Sports Buildings, p.534-549.

Yuan X, Chen L, Dong S, 2007. Prestress design of cable domes with new forms. *International Journal of Solids and Structures*, 44(9):2773-2782. https://doi.org/10.1016/j.ijsolstr.2006.08.026

Yuan XF, Dong SL, 2003. Integral feasible prestress state of cable domes. *Computers & Structures*, 81(21):2111-2119. https://doi.org/10.1016/S0045-7949(03)00254-2

Zhang A, Liu X, Li J, et al., 2012. Static experimental study on large-span cable dome structure. *Journal of Building Structures*, 33(4):54-59 (in Chinese).

Zhang G, Ge J, Wang S, et al., 2012. Design and research on cable dome structural system of the National Fitness Center in Ejin Horo Banner, Inner Mongolia. *Journal of Building Structures*, 33(4):12-22 (in Chinese).

Zhang LM, Chen WJ, Dong SL, 2007. Initial pre-stress finding procedure and structural performance research for Levy cable dome based on linear adjustment theory. *Journal of Zhejiang University-SCIENCE A*, 8(9):1366-1372. https://doi.org/10.1631/jzus.2007.A1366

Zheng JH, Luo YZ, Dong SL, et al., 2008. Model experimental research on rectangular cable dome. *Journal of Building Structures*, 29(2):25-31 (in Chinese).

Zhou JY, Chen WJ, Zhao B, et al., 2015. Distributed indeterminacy evaluation of cable-strut structures: formulations and applications. *Journal of Zhejiang University-SCIENCE A (Applied Physics & Engineering)*, 16(9):737-748. https://doi.org/10.1631/jzus.A1500081

中文概要

题　目： 双撑杆索穹顶施工成形和静力性能试验研究

目　的： 提出一种稳定性好、便于张拉施工的双撑杆索穹顶结构，以解决该结构的找力分析问题，并考察其施工方法和静力性能，为工程实践提供参考依据。

方　法： 1. 通过节点平衡方程，推导出考虑结构自重时的双撑杆索穹顶结构的预应力分布计算公式；2. 通过模型试验，比较采用空中组装和整体提升两种施工方法时，结构的内力和位形变化；3. 进行满跨荷载和半跨荷载的加载测试，并与有限元分析结果进行了对比。

结　论： 1. 本文所得公式可以准确得到双撑杆索穹顶结构考虑自重后的实际预应力分布。2. 该结构适合通过张拉外斜索施加预应力；结合整体提升的施工方法，可以显著降低施工难度，使其更适用于实际工程。3. 在外荷载作用下，双撑杆索穹顶结构中脊索和内斜索的内力减小，其他斜索和环索的内力增大。

关键词： 双撑杆索穹顶；找力分析；施工成形过程；静力性能；模型试验